

Effect of Carbon Black on UV stability of LLDPE films under artificial weathering conditions

M. Liu, A.R. Horrocks*

Faculty of Technology, Bolton Institute, Bolton BL3 5AB, UK

Received 1 October 2001; accepted 12 October 2001

Abstract

Carbon Black is recognised for its ability to stabilise polyolefins against UV degradation. Linear low density polyethylene (LLDPE) 75 μm extruded films containing a variety of carbon black with different particle size, structure and concentrations were exposed to two accelerated artificial weathering devices, a xenon arc source, e.g. Xenotest 150S, and fluorescent tube sources with UVA and UVB lamps, under controlled temperature and humidity. The changes in physicochemical properties during exposures were studied using tensile testing, Fourier transform infrared (FTIR) spectroscopic and differential scanning calorimetric (DSC) methods. Presence of each carbon black shows significant improvement in UV stabilisation compared to clear films, especially for those with small particle sizes as expected. There is no consistent effect of carbon black structure on UV stabilisation for various particle-sized carbon blacks. An increase in carbon black concentration from 1.5 to 3.5% w/w also improved UV stabilisation. For UVA and UVB sources, presence of carbon black, while increasing carbonyl group generation with respect to unit loss in tensile property with respect to unfilled LLDPE, also appears to suppress Norrish Type II scissions at photochemically generated carbonyl centers in polymer chains. This is especially the case for the smallest (20 nm) particle sizes. Thus the photostabilising efficiency of carbon black is based on both physical surface-area-dependent UV absorption and photochemical activity. Under xenon arc exposure, however, this latter is minimal. © 2002 Elsevier Science Ltd. All rights reserved.

Keywords: Polyethylene; LLDPE; Carbon Black; UV; Carbonyl; Vinyl; Photodegradation

1. Introduction

Carbon black has been an established light stabilising additive in polyolefins (and other polymers) for many years [1]. It is believed to function as a simple physical screen, a UV absorber, a radical trap and a terminator of the free radical chains through which the photo-oxidative reactions are propagated [1,2]. The resistance to UV degradation is usually related to the type and particle size of the carbon black used as well as to the concentration and dispersion of the carbon black in the matrix [3]. Small particle sized-carbon blacks are known to have the greatest UV stabilising efficiency but tend to agglomerate into aggregates or clusters which are not easily dispersed [1,4].

The complex mixture of chemisorbed, oxygenated groups on carbon black particle surfaces may also

account for their UV protective capacity [5], and the quinonic and phenolic groups present may especially function as antioxidants [6]. The understanding of the role of carbon black towards oxidation may be summarised in terms of an antioxidant effect, probably via catalytic decomposition of peroxides and free radical scavenging with greater effectiveness at low temperature, balanced by a pro-oxidant property under some conditions [7]. The observed effect of a given carbon black–polyolefin combination is the resultant of anti- and pro-oxidant effects influenced by both content and inherent properties of carbon black [8]. Recently published results [9,10] regarding the behaviour of carbon black-filled polypropylene tapes showed that the concentration, particle diameter and structural characteristics of carbon black have significant effects on the tensile and morphological properties as well as thermal and photo stabilities.

This paper discusses the first part of an investigation of the effect of a series of carbon blacks having a range of particle properties on the UV stability of linear low

* Corresponding author. Tel.: +44-1204-528851; fax: +44-1204-399074.

E-mail address: arch1@bolton.ac.uk (A.R. Horrocks).

density polyethylene (LLDPE) films (75 μm) in the absence and presence of hindered amine light stabilisers (HALS) under artificial weathering conditions. This first part investigates the effects that the particle variables of diameter, structure and volatile content have on the tensile and physicochemical structure of LLDPE films after UV exposure. Two accelerated artificial weathering devices, Xenotest 150S and Q-Panel QUV/se with UVA (315–340 nm) and UVB (280–315 nm) lamps, under controlled temperature and humidity were employed.

2. Experimental

2.1. Materials and film production

LLDPE powder used was supplied by Union Carbide (GRSN 7510NT) and is the copolymer of ethylene and hex-1-ene with density of 0.919 g/cm^3 and MFI of 0.75 $\text{g}/10$ min at 190 $^\circ\text{C}$, 2.16 kg. HPLC [carried out at Cabot Plastics (UK) Ltd.] analysis indicated that the LLDPE powder contained 0.1% (w/w) B-blend of anti-oxidant system B225 (Irganox 1010:Irgafos 168 = 1:1, Ciba Speciality Chemicals) for melt stabilisation during manufacture.

Carbon black properties are determined by their mode of manufacture and are defined in terms of their primary particle size, porosity, aggregate and surface chemical composition [11]. Carbon black particles do not exist separately but as aggregates which represent more accurately their effective size [11]. The shape or structure of these aggregates is industrially determined by the dibutyl phthalate (DBPA) absorption method [12]. Low structured blacks tend to have simple (linear or spherical) aggregated geometries, whereas highly structured blacks have complex and often branched aggregates [13,14].

In addition to the carbon black variables of particle size, structure and concentration, volatile contents that reflect the chemical compositions on the particle surfaces may be defined. However, in this study, volatile contents of selected carbon blacks are relatively low (1.0 and 1.5%), and the effect of volatile content on the UV durability is not considered. The main properties of nine grades of carbon black used at two concentrations are shown in Table 1. The various carbon blacks are grouped into small/low, medium/medium and large/high respective size/structure combinations.

The carbon black-containing LLDPE films were extruded by using Plasticisers MK1 single laboratory screw extruder with $L/D=21$ and internal barrel diameter of 22 mm through a slit die 60×0.4 mm on to a water-cooled chill roll. Edges of the films were trimmed off before collection. A cavity transfer mixer (CTM) was installed between the end of the screw and extrusion die in order to give good dispersion of carbon black in the films. Films were produced in a generally disorientated form 75 μm thick.

2.2. Artificial weathering

The exposure sources used attempt to replicate UV with shorter (UVB; 190–315 nm), longer (UVA; 315–400 nm) and total wavelength contents of the terrestrial sun spectrum. Respective irradiation times were chosen so as to be less than or at least equal to those required to generate a 50% loss of tensile behaviour for the most stable films. In practice this was difficult to achieve because of the long times needed with some sources and irradiation times of upto 4000 h for UVA, 2000 for UVB and 2400 h for xenon arc sources were found to be required.

2.2.1. UVA and UVB fluorescent tube sources

The fluorescent tube sources used in this project were either UVB lamps (310 nm maximum intensity) or UVA

Table 1
Physical properties of Carbon Black used [13,15]

Code	Concentration (%)	Nitrogen		DBPA structure ($\text{cm}^3/100$ g)	Re-grouping	
		Surface area (m^2/g)	Particle size (nm)		Particle size	Structure
C1	1.5	30	60	65	Large	Low
C2	3.5					
C3	1.5	200	18	117	Small	High
C4	3.5					
C5	1.5	130	20	98	Small	Medium
C6	3.5					
C7	1.5	210	17	68	Small	Low
C8	1.5	110	24	114	Medium	High
C9	1.5	84	25	102	Medium	Medium
C10	1.5	80	27	72	Medium	Low
C11	1.5	42	45	121	Large	High

lamps (340 nm maximum intensity) in a QUV/se tester (Q-Panel Company) consisting of two exposure chambers at each side containing four of the appropriate 1.2 m fluorescent tubes designed to give acceptably uniform outputs over their lengths except close to respective ends. The installed solar eye system via two sensors per side evenly control the exposure intensity between the horizontal tubes and also monitors the overall tube intensities. The radiation intensity was calibrated by a radiometer every 400 h. UVB radiation intensity was 0.63 W m^{-2} at a chamber temperature of $60 \text{ }^\circ\text{C}$ whilst the irradiation of UVA was set at 1.25 W m^{-2} and the same chamber temperature. In order to provide a more realistic weather exposure regime, the UVB source was also used in alternating light (8 h $60 \text{ }^\circ\text{C}$) and dark (4 h $50 \text{ }^\circ\text{C}$) with condensation mode [UVB(C)] cycles.

Two film specimens ($320 \times 90 \text{ mm}$ with total specimen exposure area of $115 \times 45 \text{ mm}$ for each of two film specimens) were mounted in each sample holder and sample holders were horizontally shifted one space laterally daily to minimise abnormal exposures as a consequence of illuminant intensity and wavelength variability along the tube lengths [16]. Previous calibration experiments had demonstrated that end positions of holders received lower radiation intensities than the others which were acceptably uniform [17]; consequently, each end sample holder was used without any specimen present.

2.2.2. Xenon arc source

The Xenotest 150S (Heraeus Ltd., UK) fitted with a 1300 W xenon arc lamp (source intensity estimated from the manufacturer's specifications for the infrared filtered condition $\sim 0.0 \text{ W/m}^2/5 \text{ nm}$ at 310 nm and $\sim 2.5 \text{ W/m}^2/5 \text{ nm}$ at 340 nm) was used in this project. Film samples were cut to fit the $135 \times 45 \text{ mm}$ specimen holders. To simulate outdoor sunlight weathering conditions, six infrared and one dark UV filters were fitted around a xenon arc lamp. The black panel temperature was set at $45 \pm 3 \text{ }^\circ\text{C}$ and the relative humidity controlled at $65 \pm 5\%$ in the exposure chamber. The xenon arc lamp was replaced after 1500 h running period as recommended by the manufacturers because of excessive and unacceptable intensity deterioration.

2.3. Characterisation

2.3.1. Tensile properties

Tensile properties of films with an average of 10 specimens per sample (except for the Xenon exposed samples where the more limited capacity allowed for only five specimens each) were obtained using an Instron Model 4300 tensile tester with a cross-head speed of 200 mm min^{-1} and gauge length of 100 mm and specimen widths of 5 mm . The tests were undertaken in an air-conditioned environment at $20 \text{ }^\circ\text{C}$ and relative humidity of 65% . Because of their disorientated character, tensile

experiments showed that strength measurements were prone to excessive error whereas results for breaking extension were more easily and conveniently determined ($< 3\% \text{ CV}$). The decision to record breaking or ultimate elongation was supported by the known sensitivity of LLDPE to UV light exposure because of the defects or cracks formed during photo-oxidative degradation and the heterogeneous character of the degradation process itself [18,19].

2.3.2. Fourier transform infrared (FTIR) spectroscopic studies

To monitor changes in polymer compositions after artificial weathering, a Mattson 3000 Unicam Fourier Transform Infrared Spectrophotometer was used. The IR spectra were recorded by plotting wavelength against absorbance from 600 to 4000 cm^{-1} wavenumbers at a resolution of 4 cm^{-1} and an average of 50 scans per specimen. In order to correct for variations in sample thickness and gain a quantitative measure of the absorbance peak intensity of the functional group, all absorbance measurements were normalised with respect to the absorbance peak at 719 cm^{-1} (CH_2 rocking band) which, as a reference, remains unchanged during the degradation processes. The ratio of the absorbance peaks at 1712 to 719 cm^{-1} and 908 to 719 cm^{-1} may be defined as carbonyl index (CI) and vinyl index (VI), respectively [20], i.e:

$$\text{Carbonyl Index} = \frac{\text{Absorbance at } 1712 \text{ cm}^{-1}}{\text{Absorbance at } 719 \text{ cm}^{-1}}$$

$$\text{Vinyl Index} = \frac{\text{Absorbance at } 908 \text{ cm}^{-1}}{\text{Absorbance at } 719 \text{ cm}^{-1}}$$

2.3.3. Differential scanning calorimetry (DSC) studies

Crystallinity, melting and post-fusion oxidative behaviours of films were measured in a Polymer Laboratories DSC thermal analyser. Each sample with a mass of $4 \pm 0.2 \text{ mg}$ was loaded in an open aluminum crucible and heated at $5 \text{ }^\circ\text{C min}^{-1}$ from ambient to $300 \text{ }^\circ\text{C}$ under flowing air at 20 ml min^{-1} . An open aluminum pan was used as a reference. The temperature and enthalpy responses were calibrated according to the known melting points and heats of transition of pure indium and tin. The area under the fusion endotherm from a DSC trace was integrated by the computer analyser to measure the heat of fusion (H_f) which is proportional to the crystallinity of a polymer. The temperature of onset of the post-fusion oxidative exotherm (T_{on}) was obtained at the point of intersection of constructed tangents as discussed elsewhere and has been reported to be a sensitive indicator of oxidation [21].

3. Results and discussion

3.1. Unexposed film properties

The summary of mechanical and morphological properties of unaged films is shown in Table 2. In general, the elongations-at-break for filled films are lower than for the pure film. Furthermore, films with a higher carbon black concentration (3.5% w/w) had slightly higher ultimate elongations than lower concentration analogues (1.5% w/w) except for the large particle-sized films (CB1 and CB2), which show comparable results.

There is essentially no difference of melting temperatures (T_m) for the unfilled and filled films and the onset

temperatures (T_{on}) of post-fusion oxidation for the filled films at concentrations of 3.5% w/w are higher than analogous 1.5% w/w filled films. This may directly represent the anti-oxidant effect of these carbon blacks [21]. The filled films generally show higher values of the heat of fusion (H_f) with respect to values for the unfilled films as the results of the nucleating effect of carbon black [22].

3.2. Effect of carbon black on elongation-at-break

3.2.1. UVB exposure

Fig. 1 shows the effect of UVB exposure time on retained breaking elongation for the unfilled and filled films containing 1.5% w/w carbon black. Significantly, the pure film shows a rapid decrease with exposure time compared to any of the carbon black-containing films. In the filled films, the small particle-sized C7 film shows the best UV resistance whilst the large particle-sized C1 and C11 films present the poorest UV resistance as expected from previous studies [3]. However, in medium particle-sized black-containing films, the loss rate of retained elongation with UVB exposure for C8 film is less than that for the C10 film. These comparative results may be quantified by determining the times for each film to lose 20% of its initial breaking elongation as listing as respective t_{20} values in Table 3. Comparing the low- and high-structured films, there is no consistent indication of effect of carbon black structure in UV stabilising effectiveness that is independent of observed particle size effects.

The expected dependence of stabilising effect on carbon black concentration is shown in Fig. 2 where C2, C4 and C6 samples represent the higher concentration (3.5% w/w) analogues of C1, C3 and C5 (1.5% w/w),

Table 2

Mechanical and morphological properties of unexposed films with and without Carbon Black

Code	Concn (%)	ε (%)	S.D.	T_m (°C)	H_f (mJ/mg)	T_{on} (°C)
LL	0	773	22	115	67.4	234
C1	1.5	717	60	113	75.3	234
C2	3.5	729	24	114	59.4	237
C3	1.5	773	21	115	66.5	238
C4	3.5	662	50	114	72.8	242
C5	1.5	760	39	116	78.6	238
C6	3.5	740	67	116	71.5	240
C7	1.5	724	29	113	73.3	237
C8	1.5	754	41	113	84.6	236
C9	1.5	771	18	113	80.1	237
C10	1.5	761	17	114	78.6	235
C11	1.5	754	14	114	76.6	237

Concn, concentration of Carbon Black; ε , elongation-at-break; S.D., standard deviation; T_m , melting temperature obtained from melting peak; H_f , heat of fusion calculated from melting endothermic area; T_{on} , onset temperature of post-fusion oxidation.

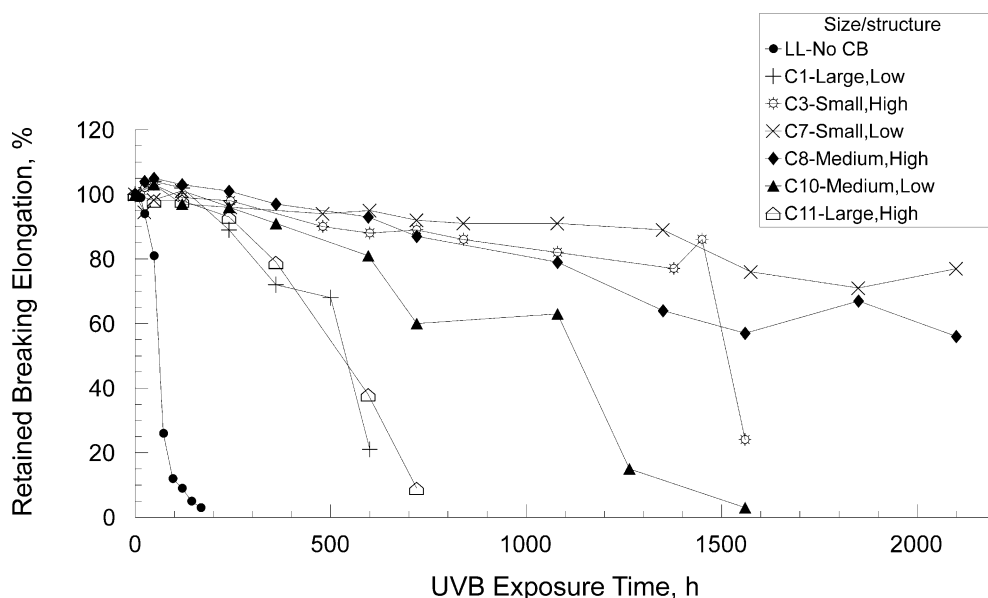


Fig. 1. Effect of UVB exposure time on retained breaking elongation.

Table 3
Times for loss of 20% of breaking elongation, t_{20} , for all film/exposure conditions

Code	Particle size (nm)	Surface area (m ² /g)	t_{20} (h)			
			UVB	UVB(C)	UVA	Xenon
LL			50	40	110	250
C1	60	30	300	340	450	440
C3	18	200	1050	1060	2100	430
C5	20	130	1000	700		520
C7	17	210	1450	1000		650
C8	24	110	1080			1600
C9	25	84	1080	1050	2200	700
C10	27	80	600	480		600
C11	41	42	350	270	500	500

respectively, as expected [3]. Again the small particle-sized C3 and C4 films show superior UVB resistance within each sample group of the same concentration and C3 film with 1.5% carbon black shows better UVB resistance than the C2 film with 3.5% carbon black.

3.2.2. UVB with condensation, UVB(C) exposure

Tensile changes only were monitored under this condition and were recorded as a function of total light exposure time to enable comparison with UVB results. The relative changes in breaking elongation with time for small (C3, C7) and high (C1, C11) particle-size-containing films with respect to each other and unfilled LLDPE films were similar to results for UVB-exposed films in Fig. 1. However, UVB(C) irradiation tends to increase degradation rates in most cases as shown from respective t_{20} values in Table 3.

3.2.3. UVA and xenon arc exposures

The generally similar trends are shown in Figs. 3 and 4 for losses in retained breaking elongation for the unfilled and filled films following UVA and xenon exposure, respectively. However, in Fig. 3, the trends of reduction in the elongation with UVA exposure are little different for small particle-sized C3 and C7 films up to 4000 h and comparable to the medium particle-sized C9 film performance. This similar behaviour for the medium particle-sized C8 film was noted in Fig. 1 with UVB exposure. Generally, for LL and carbon black-filled films, UVA exposure yields t_{20} values (see Table 3) almost twice those for respective UVB-degraded films supporting the general understanding that at similar intensities, longer wavelength UV is less damaging [23].

One feature of interest for xenon arc-exposed samples (see Fig. 4) is the lower level of trend smoothness and the scatter of data points particularly for the C3 film. Furthermore, the carbon black-filled film curves suggest less of an apparent general stabilising effect with respect to LL film than observed for UVA- and UVB-degraded films. Surprisingly and as might not be expected for exposure by the generally longer wavelength characteristics of the xenon source (ignoring intensity effects), its poorer degrading efficiency of LL film, as indicated by respective t_{20} values (see Table 3) is not reflected consistently in black-filled film performance. For small particle-size black containing films (C3, C5 and C7), lower t_{20} values are apparent with respect to UVA and UVB results. For the higher structured blacks in C8 and C11, medium and large particle-sized films, t_{20} values have increased relative to UVB exposure performance suggesting a positive effect of high structure against a

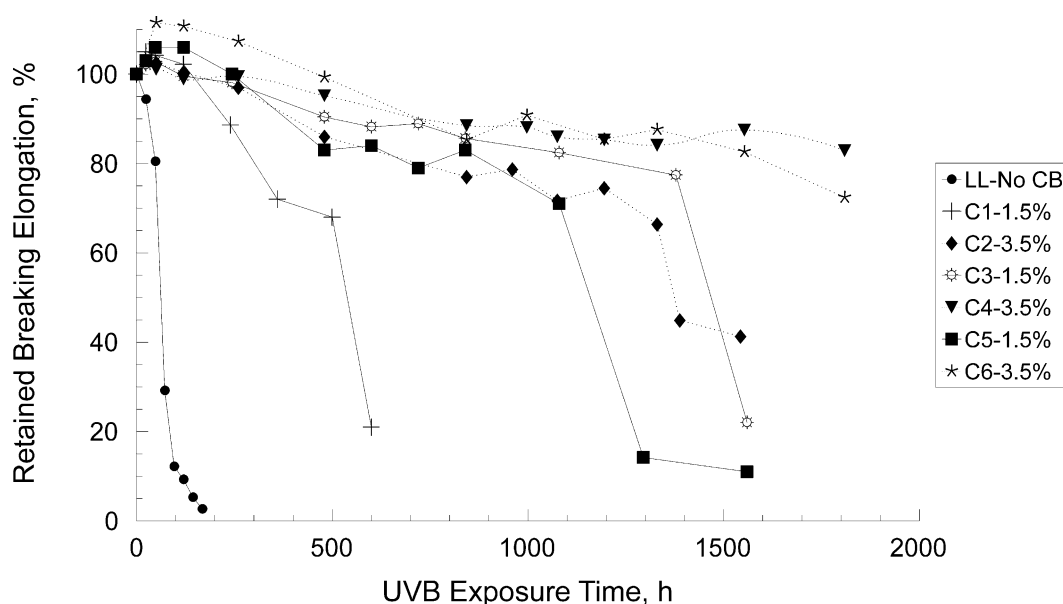


Fig. 2. Effect of CB concentration on retained breaking elongation.

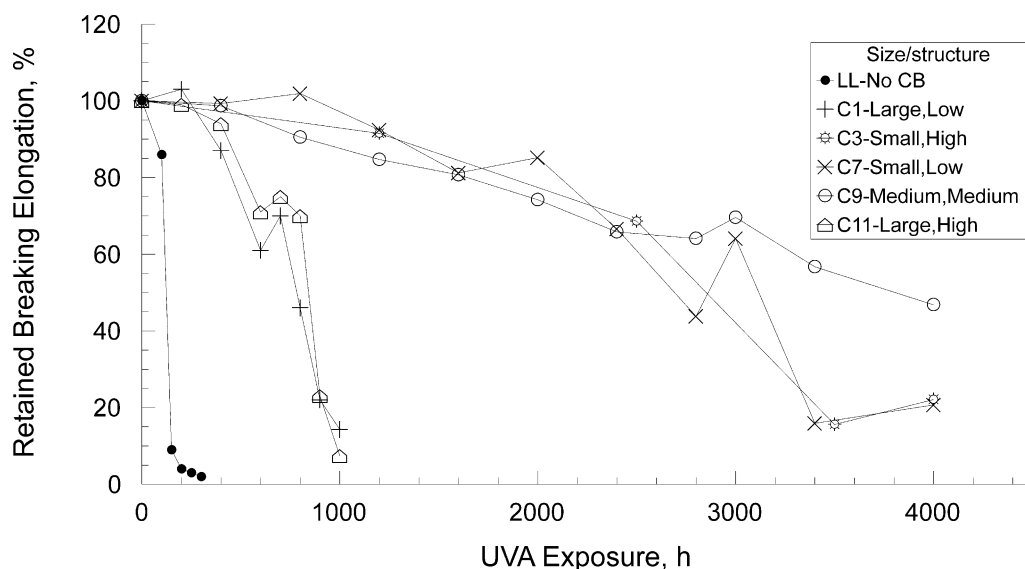


Fig. 3. Effect of UVA exposure on retained breaking elongation.

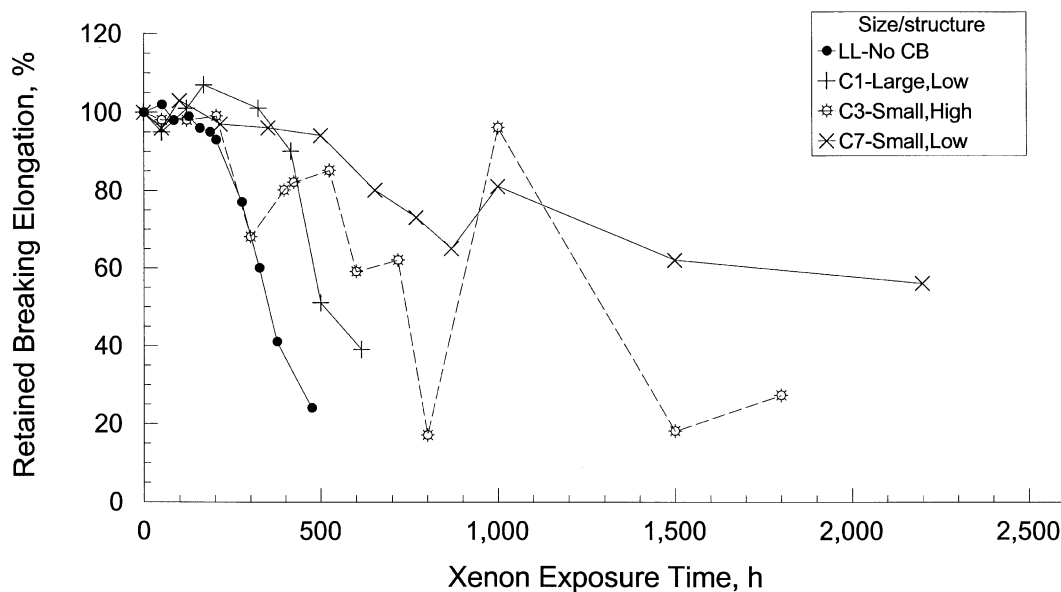


Fig. 4. Effect of xenon exposure on retained breaking elongation.

background of generally poorer stabilising effectiveness. C8 and C9 (medium particle size) and C1 (large particle size) show variable behaviour relative to UVB results.

3.3. Effect of carbon black on the formation of functional groups

It is well known [20] that photo-oxidative degradation of polyolefins is a consequence of photochemical processes involving generation of and attack by free radicals of the polymer chain causing chain scission and generation of functional groups. The main changes in the infrared spectrum are located in the areas of 3100–

3700, 1600–1900 and 800–1000 cm^{-1} which are associated with the formation of hydroperoxides, carbonyl groups and unsaturated groups, respectively.

3.3.1. UVB exposure

As recorded FTIR spectra show [17], there are increases with exposure time in the maximum absorption peaks at 3605 cm^{-1} from free hydroperoxide, at 3431 cm^{-1} from associated hydroperoxide, at 1736 cm^{-1} from ester, at 1712 cm^{-1} from ketone, 908 cm^{-1} from vinyl and at 887 cm^{-1} from vinylidene groups. However, the spectral responses between 3100–3700 cm^{-1} show greater noise levels for the filled than the pure

film, probably due to the result of the high optical density of carbon black. The distinctive peak at IR spectra of 3371 cm^{-1} for the pure film is absent for the filled films and the greater width of the absorption band between 1712 and 1732 cm^{-1} for filled films may be attributed to the overlapping of a population of similar $>\text{C}=\text{O}$ -containing moieties which might be associated with a number of oxygenated groups on carbon black particle surfaces.

Carbonyl and hydroperoxide groups have been recognised as two of the important groups for the investigation of photo-oxidation of LLDPE [24]. The increases in normalised absorbances of associated hydroperoxide at 3431 cm^{-1} and ketonic groups at 1712 cm^{-1} with exposure time are shown in Figs. 5 and 6, respectively. As expected, the unfilled film shows dramatic

increases in the absorbance indices of both functional groups with UV exposure time compared to the filled films. The large particle-sized C1 and C11 films show the fastest rates of increase in the formation of these groups among the filled films. The C7 film containing small particle-sized carbon black shows the slowest formation of the associated hydroperoxide and carbonyl groups which would indicate the best UV resistance; this is confirmed by its superior elongation-at-break properties in Fig. 1. However, it is evident that even for C7 film, carbonyl levels after 2100 h exposure, equivalent to 20% loss in breaking elongation, are higher than comparable degraded LL film levels. Table 4 lists estimates of respective carbonyl group induction periods, t_i to the nearest 10 h.

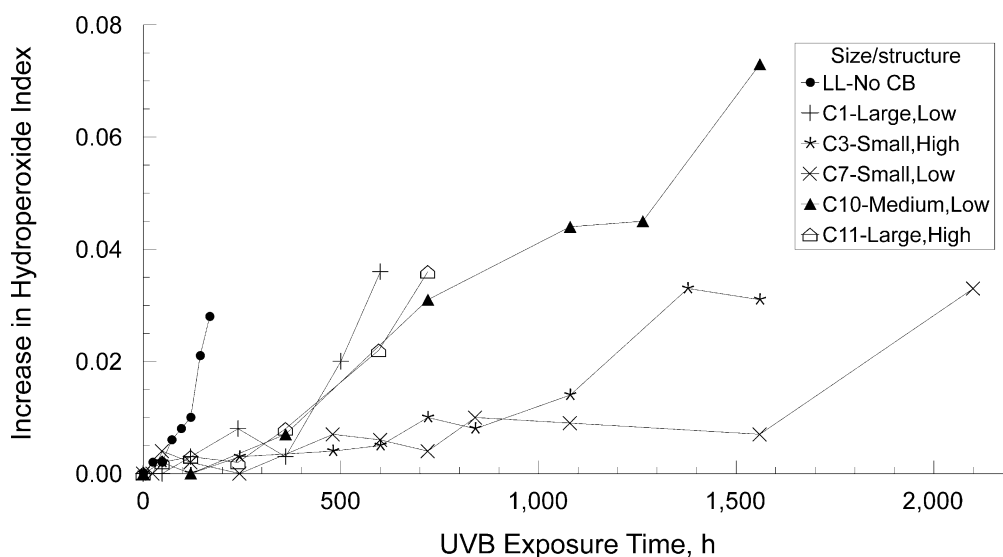


Fig. 5. Effect of UVB exposure on hydroperoxide index.

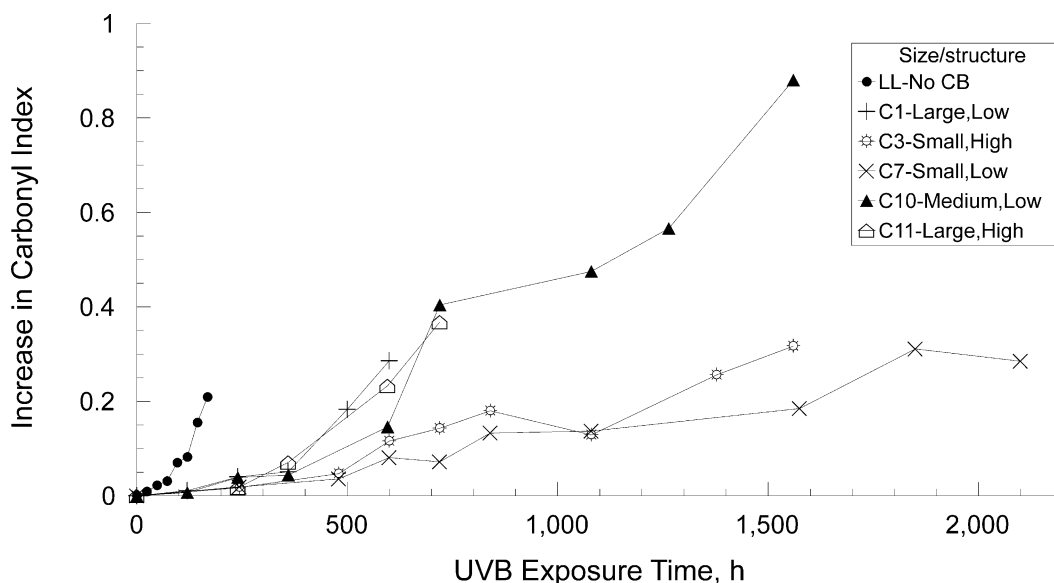


Fig. 6. Effect of UVB exposure on carbonyl index.

Table 4
Induction times, t_i , for carbonyl group formation

Particle size	Structure	Code	Induction time, t_i (h)		
			UVB	UVA	Xenon
Small	Low	C7	500	1200	450
	Medium	C5	600		
	High	C3	480	1200	200
Medium	Low	C10	600		
	Medium	C9	400	1200	
	High	C8	400		
Large	Low	C1	360	700	270
	High	C11	360	700	200
Unfilled		LL	70	150	180

According to known primary photochemical reaction mechanisms, Norrish Type II scissions of photo-generated carbonyl groups lead to the formation of both new carbonyl and vinyl groups [25]. Fig. 7a shows the general increases in VI at 908 cm^{-1} with UVB exposure time. It is obvious that for all filled films, no matter what differences in carbon black physical properties, the generation of vinyl groups show very low rates of increase which seem to level off after relatively longer exposures. These phenomena may be explained by carbon black depressing Norrish Type II reactions during photo-oxidation of the filled films.

3.3.2. UVA exposure

Very similar changes in the various functional group behaviour occurs for unfilled and filled LLDPE films. As expected, respective rates of group absorbance change per unit time are less than seen for the shorter wavelength UVB irradiated samples and Table 4 presents the respectively longer carbonyl induction times (to the nearest 50 h). An almost doubling in t_i for a given film reflects the similar effects on respective t_{20} values in Table 3. Again, the more stabilising small particle-sized blacks in C3 and C7 films show lower rates of absorbance increase for hydroperoxide (3431 cm^{-1}) and carbonyl (1712 cm^{-1}) groups than medium (C10) and large (C1, C11) particle-sized black-containing films. Furthermore, suppression of vinyl absorbance (908 cm^{-1}) is almost total during UVA irradiation as Fig. 7b shows. It may thus be assumed that the longer wavelength UVA irradiation completely suppresses Norrish Type II reactions and the associated losses in mechanical properties in Fig. 4 occur without formation of vinyl groups.

3.3.3. Xenon arc exposure

The presence and behaviour of the hydroperoxide, carbonyl, vinyl and vinylidene group absorptions behave similarly to those in UVA- and UVB-exposed films and like the filled UVA-exposed films, vinyl group

absorption change is negligible. Again, the increase in hydroperoxide formation (at 3431 cm^{-1}) shows no induction periods but unlike for UVA- and UVB-exposed films (see Fig. 5 for UVB exposures), presence of carbon black does not show a marked rate-reducing effect. In fact, filled films appear to exhibit higher rates of -OOH formation. However, as seen for other films, induction periods for carbonyl group formation at (1712 cm^{-1}) do increase in the presence of carbon black as shown in Table 4 with C7 having the greatest effect. Of greatest surprise, however, is the observation in Table 4 that t_i values for carbonyl group formation are shorter than those for even UVB-exposed films reflecting their equally surprisingly low t_{20} values for small (C3, C5, C7) and some medium (C9, C10) sized blacks.

3.4. Effect of carbon black on crystallinity

The effects of UVB exposure on crystallinity derived from DSC of exposed films and expressed as heat of fusion are shown in Fig. 8. Photochemically induced chain scissions at the slightly elevated exposure temperature at $60\text{ }^\circ\text{C}$ may enable restructuring and re-crystallising of the films to occur during exposure [19]. At longer exposure times, the increased crystallinity often results in the surface cracking. The combination of the scission of inter-crystalline bonds and stress concentration at surface cracks leads to crack propagation as the dominant mechanism of polymer degradation [26]. For the pure film, an increase in crystallinity is clearly seen with increasing exposure time. However, for the filled films, the crystallinity initially increases and tends to constant values within a range of $80\text{--}110\text{ J/g}$ during exposure; this effect seems to be independent of the physical properties of carbon black. The filled films already have slightly higher crystallinities (see Table 2) because carbon black acts as a nucleating agent and this effect may continue following initial photolytic or oxidative chain scission to a final equilibrium value where further crystallisation may be hampered by the dispersed particle-polymer domains present interfering with the growth of microcrystalline aggregates.

UVA-exposed films behave in a similar manner to the results shown in Fig. 8 for UVB exposures although crystallinity decreases appear to occur for large (C1) and small (C7) particle-sized films after 1000 h exposures. This suggests that chain scission with a concomitant reduction in order dominates at longer exposure times as might be expected. Careful inspection of UVB-exposed results in Fig. 8 also suggest that large (C1, C11) and medium (C10) particle-containing films are starting to show reductions in DSC-derived crystallinity above 1200 h.

Independently obtained X-ray diffraction measures of crystallinity obtained at the University of Newcastle (Phillips PW 1730 diffractometer, Cu K_α radiation) are

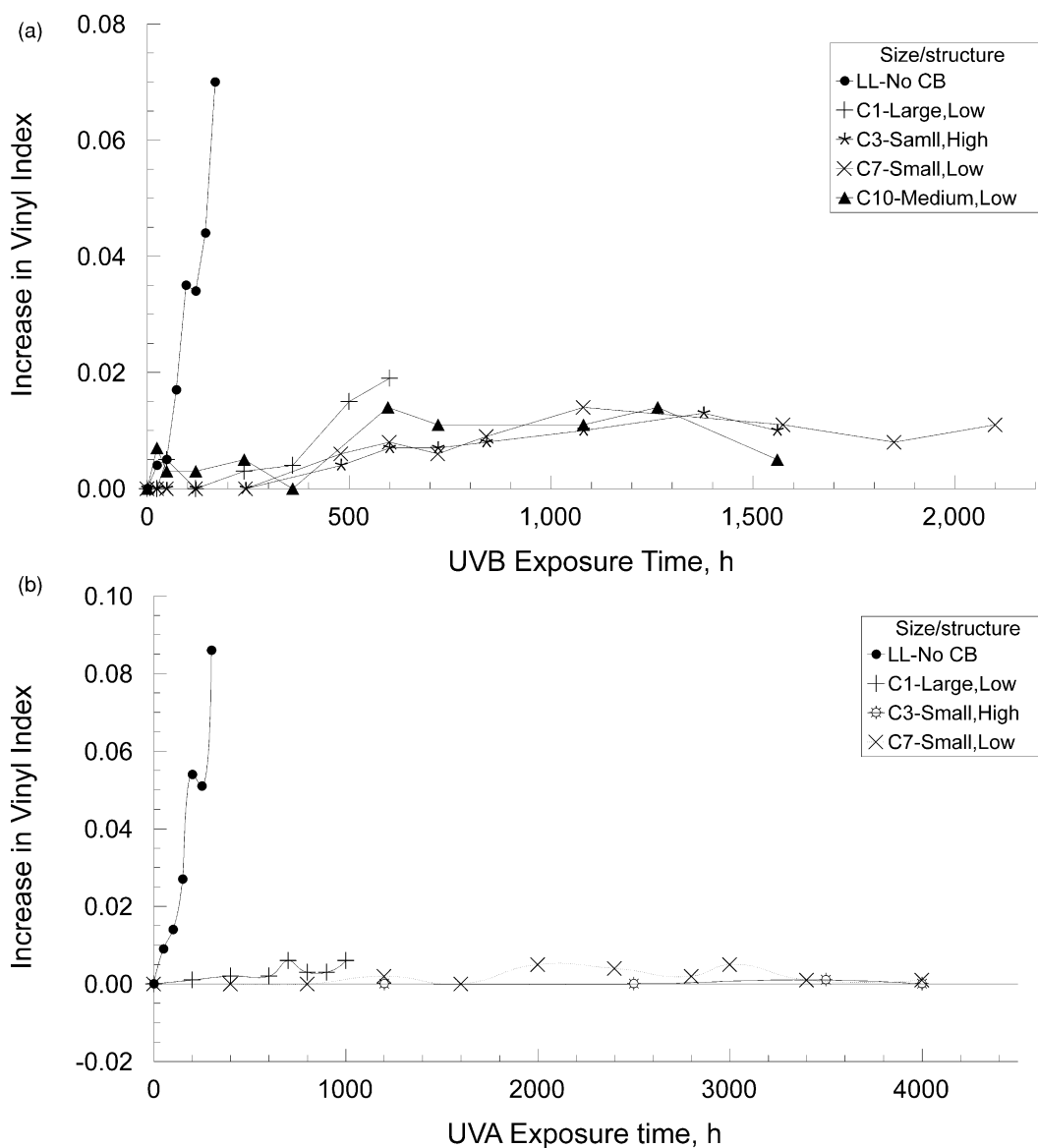


Fig. 7. Effect of UVA and UVB exposure on vinyl index.

shown in Fig. 9 for UVB-exposed films. The trends shown compare well with those in Fig. 8 except that values tend to asymptote to crystallinity index values [27] within the 80–83% range. Decreases seen in the DSC-derived values are not apparent thereby suggesting that observed changes in shapes of fusion endotherms during longer UV irradiation times reflect not only changing overall order but in the distribution of the polycrystallinity and so integrated values may not simply relate to the former.

3.5. Comparison of effects of various UV sources

Comparison of the results for the pure LLDPE film, shows that the UV degradative effects in terms of time-dependence of breaking elongation may be expressed in the order of xenon < UVA < UVB < UVB(C) as shown

in Fig. 10. The more severe UV degradation occurred under the UVB(C) condition may be a consequence of dark reactions occurring under a warm moist environment during the condensation cycle which enhances the effect of subsequent UVB deterioration. Apart from the effect of moisture it is shorter wavelength radiation that causes more damage of the unfilled film during UVB (280–315 nm) exposure compared with UVA (315–400 nm) exposure as previously suggested [24,26], even though the UV intensity of UVA source used is higher than that of UVB source.

As discussed above and shown in Table 3 for sample t_{20} values, the relative degradative effect of the UV sources on the large particle-sized black (C1 and C11) films generally is in the order of xenon \sim UVA < UVB \leq UVB(C). This order, while being similar to that for unfilled films, is different to the increasing sequence

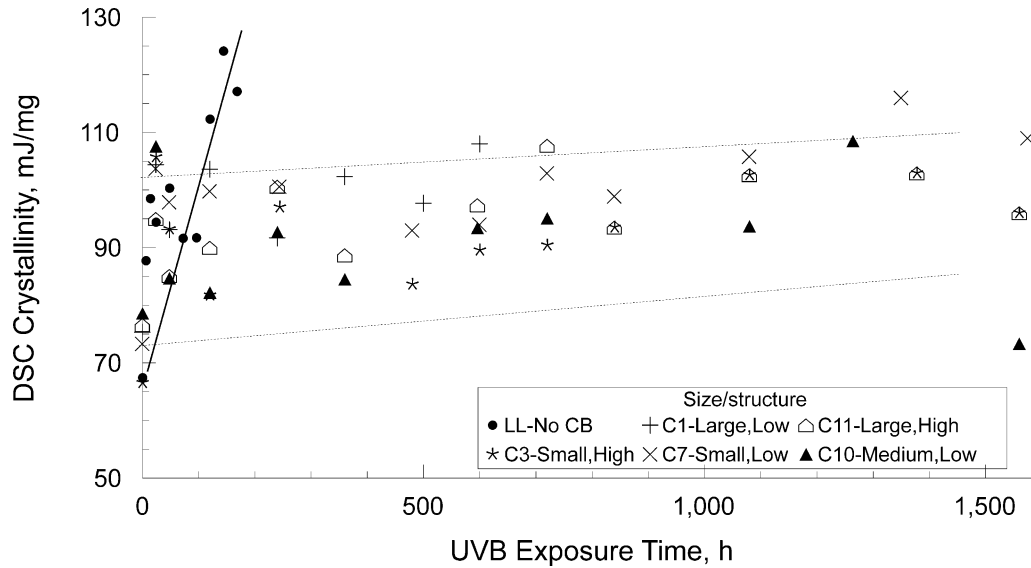


Fig. 8. Effect of UVB exposure on crystallinity.

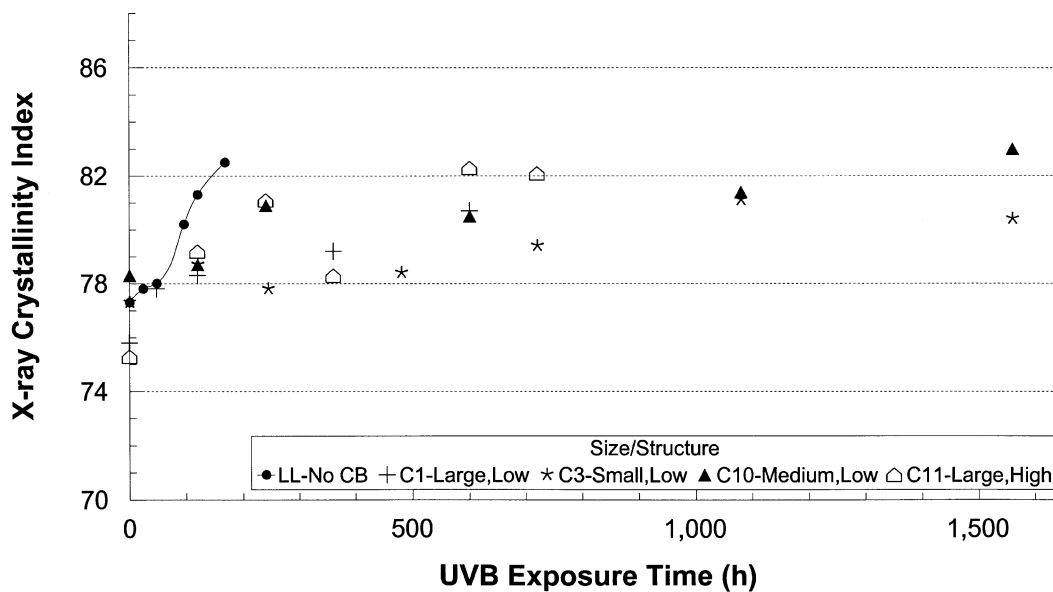


Fig. 9. Effect of UVB exposure on X-ray-derived crystallinity.

UVA < UVB ≤ UVB(C) < Xenon for the small particle-sized black-containing (C3 and C7) films and the medium particle-sized C9 films. This increased apparent severity of the xenon source is especially interesting for the most stabilising carbon blacks, given its less damaging effect on unfilled LLDPE films (see Fig. 10). Generally, of the four UV sources, the UVA exposure conditions show the least damage to the filled films which suggests that the 340 nm wavelength region alone poses a lesser UV hazard. However, the carbon black particles, especially those with smallest particle size and highest surface areas, will absorb all xenon spectral wavelengths through the visible and into the near IR. Much of this radiation will be degraded to heat and it is

possible that high localised temperatures above the general black panel temperature of 45 °C will ensue as indeed has been demonstrated previously by Schneider [28]. Thus it is likely that UV degradation is supplemented by thermal degradation. Finally, results in Table 3 also suggest that carbon black-induced increases in t_{20} values may be a consequence of increased particle aggregate surface areas, a point that will be explored further below.

Comparing CI increases for UVA and UVB exposures for the pure film and C1 and C3 black-containing films shown in Fig. 11 suggests that the UVB exposure conditions give faster increases in the CI than the UVA exposure conditions for all three types of films as

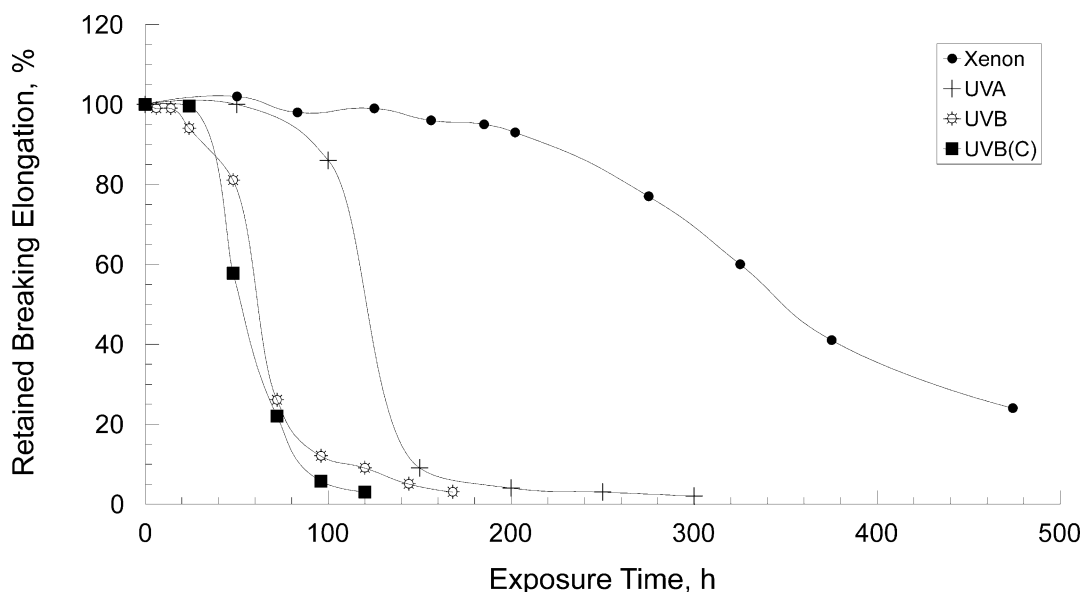


Fig. 10. Effect of various exposure sources on elongation of LLDPE film.

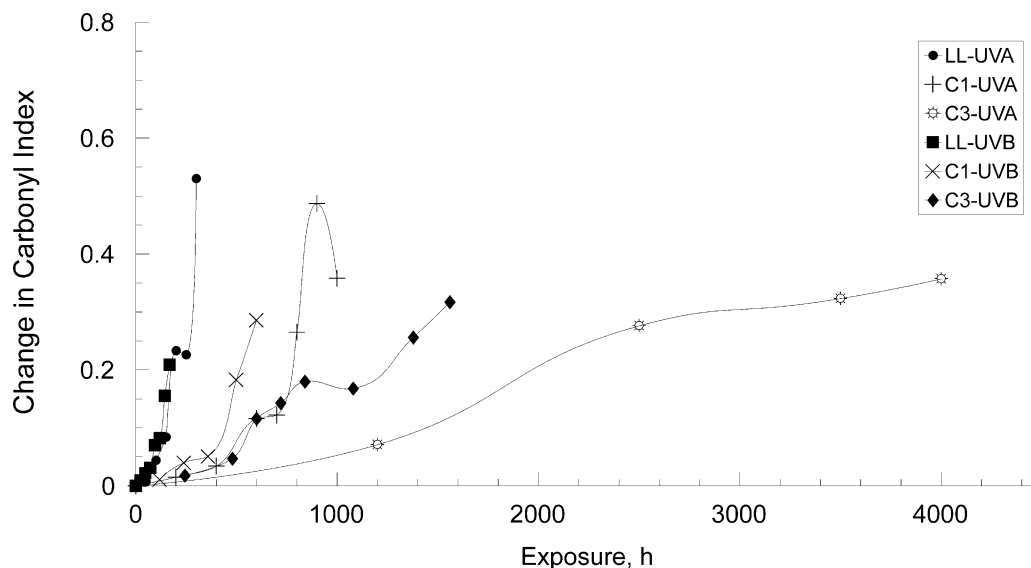


Fig. 11. Effect of UVA and UVB on carbonyl index.

expected and as indicated from induction period magnitudes in Table 3. This order corresponds to that for tensile property results in Table 3. Under either UVB or UVA exposure conditions, the increase rate of CI with exposure time still follows the order of decreasing rate: LLDPE film > C1 (large particle size) film > C3 (small particle size) film. However, xenon arc irradiation gives the shortest induction periods for $>C=O$ for all filled films tested (see Table 4).

3.6. Possible effects of carbon black variables on photostabilising mechanism

In order that a possible mechanism of the photostabilising effect of carbon black used may be proposed,

the experimental results from tensile and FTIR studies under UVB exposure conditions are analysed further in Table 5 where induction time, times for 20% (t_{20}) and 50% (t_{50}) loss of retained elongation and their respective carbonyl indices, CI_{20} and CI_{50} are collated from Tables 3 and 4 where relevant and listed. Again it is seen that these latter values are much higher for carbon black-containing films than for LL film in spite of having lost the same percentage tensile property.

The parameter t_{50} normally is the critical failure indicator for polymer films. However, it was considered overly time-consuming to obtain the t_{50} values for the small particle-filled films and so only the t_{20} values are available for all films. Fig. 12 shows the plots of exposure times to t_{20} and available t_{50} values against carbon

Table 5
UVB exposure time of 20 and 50% loss of ultimate elongation and their corresponding carbonyl index values

Code	Particle size (nm)	Surface area (m ² /g)	t ₂₀ , (h)	t ₅₀ , (h)	CI ₂₀	CI ₅₀	t _i , (h)
LL			50	60	0.047	0.055	70
C1	60	30	300	540	0.048	0.145	360
C3	18	200	1050	1550	0.13	0.31	480
C5	20	130	1000	1100	0.26	0.26	600
C7	17	210	1450	>2200	0.175	>0.285	500
C8	24	110	1080	>2200	0.21	>0.463	400
C9	25	84	1080	>2200	0.19	>0.356	400
C10	27	80	600	1100	0.15	0.37	600
C11	41	42	350	540	0.062	0.20	360

t₂₀, t₅₀, Exposure time at 20 and 50% loss of retained elongation respectively; CI₂₀, CI₅₀, carbonyl index at time of 20 and 50% loss of retained elongation, respectively; t_i, induction time at which rapid formation of carbonyl groups started.

black surface areas from Table 1. Even though all t₅₀ values have not been obtained, increasing trends with particle surface area of carbon black and hence reduced particle size are evident at both degradation conditions.

In an attempt to correlate tensile property and chemical changes, retained elongations are plotted against CI values for the unfilled and filled films under UVB exposure in Fig. 13. The presence of carbon black, while increasing the durability of films, also increases concentrations of >C=O groups present at each retained elongation value, which suggests that it does in fact have a chemical mechanistic stabilising effect in addition to the obvious physical UV-absorbing effect. The induction times, t_i for significant increases in carbonyl group formation (see Table 4) coincide with the exposure times for about 90% retention of elongation for C3, C7 films, 80% for C10 film, 70% for C1 film and

25% for the pure film. This agrees to some extent with the results in Fig. 6 where >C=O formation rate is less for the small-sized black-containing films.

These findings contradict our earlier suggestion made for the pure LDPE films [19] that the rapid formation of carbonyl groups with respect to elongation retention indicates low UV durability. Thus in LLDPE, while the UV stabilising ability of a given carbon black shows a retention of physical properties, this is accompanied by increase in the respective formation rate of carbonyl giving rise to an increase in the rate of carbonyl group formation per unit loss of retained breaking elongation. It would seem, however, that such >C=O formation is not a sensitizer of chain scission.

However, this effect is more complex than Fig. 13 suggests. With increasing surface areas, as Fig. 14 shows, the corresponding carbonyl indices, CI₂₀ and CI₅₀ at t₂₀ and t₅₀ times respectively show increases only up to the surface area value of about 130 m²/g (equivalent to 20 nm particle size) followed by sudden decreases. Thus it would seem that formation of carbonyl groups for the carbon black-containing films is dependent on carbon black surface area only up to values of 130 m²/g. Therefore, only for very small particle-sized blacks with diameters less than 20 nm, is the photochemical UV-absorbing stabilising effect accompanied by some photochemical suppression of carbonyl group formation in spite of the general tendency of all carbon blacks to photosensitise >C=O generation.

Furthermore, it has been concluded that reduction in vinyl group formation suggests that the carbon black surface reduces the possibility of Norrish Type II scissions of those photosensitive >C=O groups present. Fig. 15 shows the relationship between vinyl and carbonyl indices and it is clearly seen that for filled films

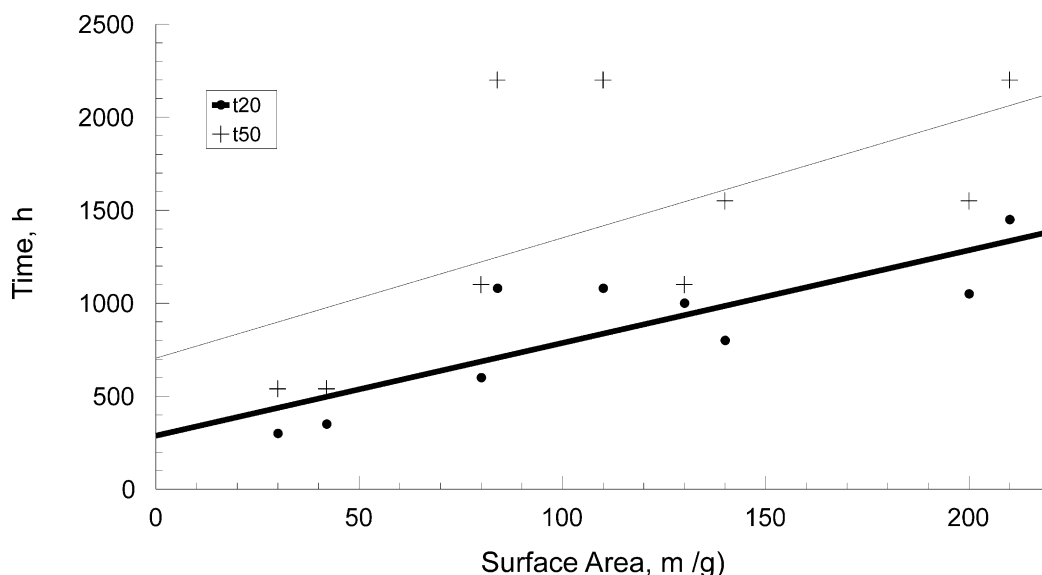


Fig. 12. Effect of surface area on times to lose 20 and 50% breaking elongation for UVB exposed samples; highest t₅₀ points are >2200 h.

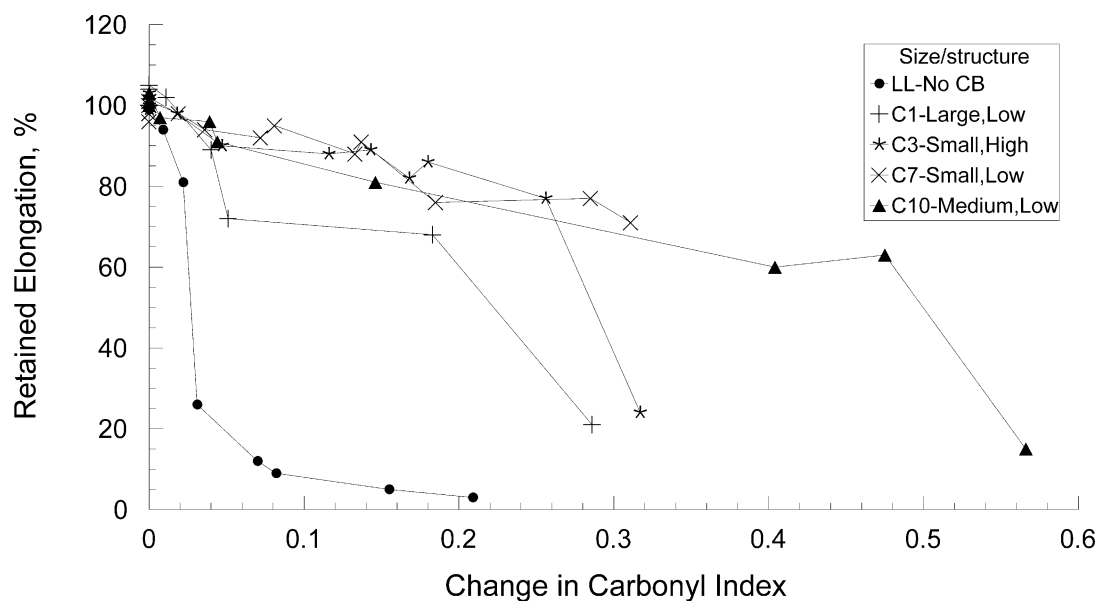


Fig. 13. Relationship of retained breaking elongation and carbonyl index after UVB exposure.

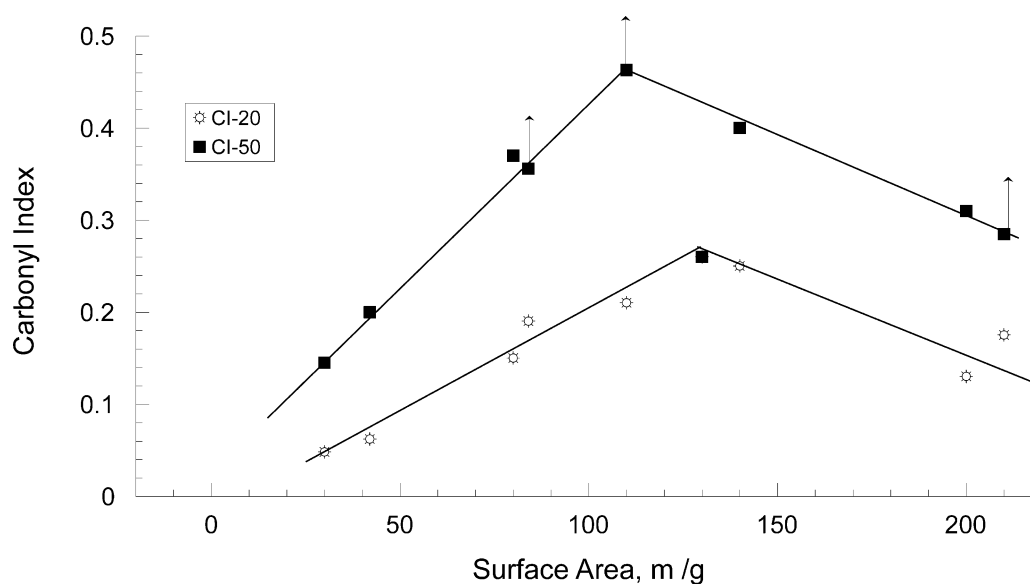


Fig. 14. Effect of surface area on carbonyl index values at t_{20} and t_{50} for UVB-exposed samples; arrowed CI-50 points should be higher since these are 2200 h data.

the latter increases independently of the former under UVB and UVA exposure.

A similar analysis of UVA data shows again that t_{20} and t_{50} increase linearly with particle surface areas and that the CI_{20} and CI_{50} rise to maxima at 120–130 m^2/g surface area similar to trends in Fig. 14. Furthermore, plots of retained breaking elongation versus CI for UVA-exposed clear and filled films show similar trends to those in Fig. 13 for UVB exposure [29]. It would seem, therefore, that the reduced Norrish Type II hypothesis holds true for UVA exposure conditions as well.

Under xenon arc irradiation, however, there appears to be no sensible relationship between either t_{20} or t_{50} and surface area, although on the whole small particle-sized blacks and C7 in particular, yield one of the highest t_{50} values >2400 h [17]. Furthermore, while CI induction times are easily measured (Table 4), rising trends following subsequent exposure were not regular making CI_{20} and CI_{50} determination difficult. The previously suggested concurrent thermal degradation occurring is likely to add to this error. In general, rates of formation were in the order $C1 > C11 > C3 > C7$. Of greatest interest are the retained breaking elongation

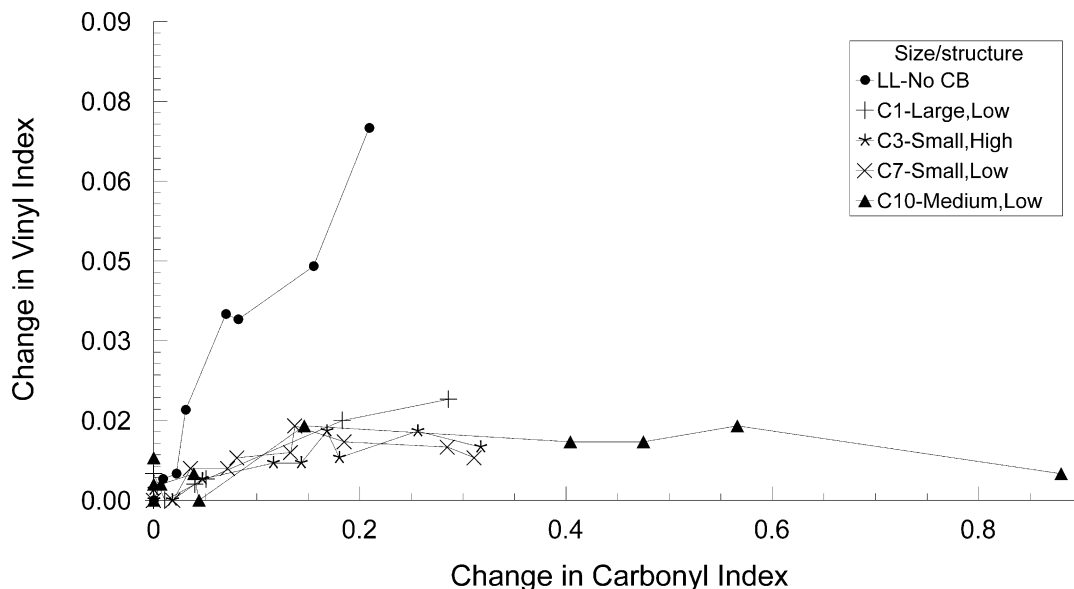


Fig. 15. Relationship of vinyl and carbonyl index after UVB exposure.

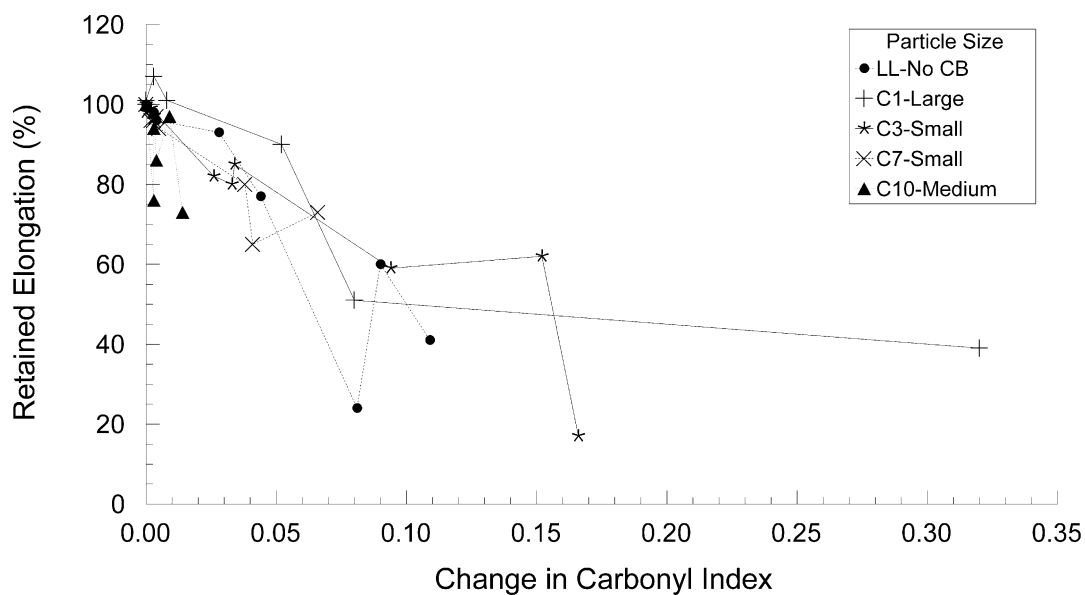


Fig. 16. Relationship between retained breaking elongation and carbonyl index after xenon arc exposure.

versus CI plots in Fig. 16 which suggest that, within error, the trends are identical and independent of whether carbon black is present or not. It would seem that now carbon black is behaving purely as a physical UV shield than whether or not carbon black stabilizes via Norrish Type II scission suppression, depends on the wavelength of incident UV. Clearly, further work is required to address this issue.

Finally, since ketonic groups absorb below 350 nm, it may be assumed that the higher intensities of the shorter wavelength components notably at 310 and 340 nm in UVB and UVA sources, respectively, will excite them and most likely promote efficient photochemical reac-

tions. While such reactions will normally favour formation of carbonyl groups via subsequent Norrish Type I and II scissions, presence of adjacent carbon black surfaces appears to quench the latter. Recent work by Allen and coworkers [30] has demonstrated that indeed carbon black pigments can be most effective quenchers of excited states.

4. Conclusions

The presence of carbon black shows significant improvement in UV durability of the extruded LLDPE

films, especially those with small particle sizes. The small and medium particle-sized black films show much more delay in loss of ultimate elongation with UV exposure than the large particle-sized black films. There is no consistent effect of carbon black structure on UV stabilisation for various particle-sized carbon blacks. As expected, the increases in carbon black concentration from 1.5 to 3.5% w/w for the filled films result in an increase in UV resistance. The losses of retained breaking elongation are accompanied by the formation of hydroperoxide and carbonyl groups. However, at the times for defined retained elongation values, e.g. t_{20} and t_{50} , the small particle-sized black films have higher values of CI in contrast to the suggestion that the formation of carbonyl group is a consequence of free radical attack on the backbone of macromolecules and chain scissions resulting in the loss of tensile property as reported for pure LDPE films [19]. The UV stabilising ability of carbon black is associated with both the UV absorbing capacity of carbon black and for UVA and UVB radiation, possibly via reduction in Norrish Type II scissions of chemisorbed and photogenerated ketonic species present on particles. This latter is especially efficient on particles having surface areas in excess of 130 m²/g which corresponds to particle diameters of 20 nm or less. In subsequent publications, the addition of Hinder Amine Light Stabiliser (HALS) to the carbon black-filled films will be examined and the combined effect of carbon black and HALS on UV stability of LLDPE films will be reported.

Acknowledgements

The authors wish to thank Cabot Corporation, Billerica, USA for financial and technical support during this research and to Dr. J. White of the University of Newcastle for use of his X-ray diffraction equipment.

References

- [1] Hawkins WL, Worthington MA, Winslow FH. *Rubber Age* 1960;88:279–83.
- [2] Hawkins WL. *Rubber Plast Weekly* 1962;142:291–9.
- [3] Wallder WV, Clarke WJ, Decoste JB, Howard JB. *Ind Eng Chem* 1950;42:2320–5.
- [4] Howard JB, Gilroy HM. *Polym Eng Sci* 1969;9(4):286–94.
- [5] Schonhorn H, Luongo JP. *Macromolecules* 1969;2:364–6.
- [6] Gruver JT, Rollmann KWJ. *Appl Polym Sci* 1964;8:1169–83.
- [7] Mwila J, Mirafat M, Horrocks AR. *J Polym Degrad Stab* 1994; 44:351–6.
- [8] Rotschova J, Pospisil J. *Angew Macromol Chem* 1992;194:201–11.
- [9] Horrocks AR, Mirafat M, Mwila J, De Groot MB, Den Hoedt G, Termat RJ, editors. *Geosynthetics: applications, design and construction*. Rotterdam: Balkema; 1996. p. 851–8.
- [10] Horrocks AR, Mwila J, Mirafat M, Liu M, Chohan SS. *Polym Degrad Stab* 1999;65:25–36.
- [11] Accorsi J, Romero E. *Plast Eng* 1995;52(4):29–32.
- [12] HEss WM, Herd CR, Donnet J, Bansal RC, Wang M, editors. *Carbon Black*, 2nd ed. New York: Marcel Dekker; 1993. p. 116 [Chapter 3].
- [13] Anon. Cabot Corporation North American Technical Report S-136.
- [14] Herd CR, McDonald GC, Hess WM. *Rubber Chem Technol* 1991;65:1.
- [15] Anon. Cabot Corporation North American Technical Report S-114, 1987.
- [16] ASTM G53-88. Standard practice for operating light- and water-exposure apparatus (Fluorescent UV-condensation type) for exposure of nonmetallic materials, 1988.
- [17] Liu M. PhD thesis, University of Manchester, UK, 1997.
- [18] Raab M, Kotulak L, Kolarik J, Pospisil J. *J Appl Polym Sci* 1982;27:2457–66.
- [19] Liu M, Horrocks AR, Hall M. *J Polym Degrad Stab* 1995; 49:151–61.
- [20] Lacoste J, Carlsson DJ. *J Polym Sci* 1992;30:493–500.
- [21] Horrocks AR, Mwila J, Liu M. In: Rita AT, Patterson GH, editors. *Oxidative behaviour of materials by thermal analytical techniques*. ASTM STP 1326. American Society for Testing Materials, 1997.
- [22] Lin Y, Zhou J, Spruiell JE. *ANTEC* 1991. p. 1950.
- [23] Davis A, Sims D. *Weathering of polymers*. London: Applied Science; 1983. p. 119 [Chapter 6].
- [24] Lacoste J, Carlsson DJ, Falicki S, Wiles DM. *Polym Degrad Stab* 1991;34:309–23.
- [25] Ranby B, Rabek JF. *Photodegradation, photo-oxidation and photostabilisation of polymers*. London: John Wiley & Sons; 1975. p. 42 [Chapter 2].
- [26] Allen NS. *Trends in Polymers* 1992;2(11):366–75.
- [27] Culleston DL, Ellison MS, Aspland JR. *Text Res J* 1991;61:594–606.
- [28] Schneider H. In: Den Hoedt G, editor. *Geotextiles, geomembranes and related products*. Rotterdam: Balkema; 1990. p. 723.
- [29] Grossman DM. The Q-Panel Company report, U-821, November 1989.
- [30] Pena JM, Allen NS, Edge M, Liauw CM, Roberts I, Valange B. *Polym Degrad Stab* 2000;70:437.